Modeling "Wrong Side" Failures Caused by Geomagnetically Induced Currents in Electrified Railway Signaling Systems

C. J. Patterson[1], J. A. Wild[1], and D. H. Boteler[2]

[1]Department of Physics, Lancaster University, Lancaster, UK
[2]Natural Resources Canada, Ottawa, Ontario, Canada

Key Points:

- A model has been extended to examine "wrong side" failures caused by space weather in DC signaling systems on AC-electrified railways
- "Wrong side" failures occur when the line is subjected to electric fields that are expected to arise once every one or two decades
- The threshold electric field for "wrong side" failures is lower than for "right side" failures

---

Corresponding author: Cameron Patterson, `c.patterson2@lancaster.ac.uk`

Abstract

The majority of studies into space weather impacts on ground-based systems focus on power supply networks and gas and oil pipelines. The effects on railway infrastructure remain a sparsely covered aspect even though these system are known to have experienced adverse effects in the past as a result of geomagnetic activity. This study extends recent modeling of geomagnetic effects on DC signaling for AC-electrified railways in the UK that studied "right side" failures in which green signals are turned to red. The extended model reported here allows the study of "wrong side" failures where red signals are turned green: a failure mode that is potentially more dangerous. The results show that the geoelectric field threshold at which "wrong side" failures occur is lower than for "right side" failures. This misoperation field level occurs on a timescale of once every 10 or 20 years. We also show that the estimated electric field caused by a 1-in-100 year event would cause a significant number of "wrong side" failures at multiple points along the railway lines studied.

Plain Language Summary

Space weather refers to the conditions and variations in the Sun-Earth environment that affect technological infrastructure both in space and on the ground. Previous studies show that railways in various countries have been affected by space weather, whereby geomagnetic interference in signaling systems leads to the display of erroneous signals. The disruption in signaling can happen when geomagnetic disturbances induce electric currents in the rails that interfere with the electrical circuits used to detect trains. This research builds upon an earlier model that assessed the effects of geomagnetically induced currents on railway signaling systems in the United Kingdom, providing the opportunity to examine new failure modes. The results show that "wrong side" failure (the potentially hazardous type of misoperation), where red signals are turned green, can occur in the line when a geomagnetic storm with frequency of about one or two decades occurs. We also demonstrate that a 1-in-100 year extreme event could cause many misoperations throughout the line in both directions of travel.

1 Introduction

Space weather has the potential to affect ground-based and space infrastructure, causing interference and/or damage. Among the many hazards associated with space weather, geomagnetically induced currents (GICs) are a significant concern. During geomagnetic disturbances, fluctuations of ionospheric and magnetospheric currents cause variations in the magnetic field observed at the Earth's surface. These variations in the magnetic field induce electric currents in the Earth and in long conductors such as power grids (Pirjola, 1985; Boteler & Pirjola, 2019; Lewis et al., 2022), oil and gas pipelines (Pulkkinen et al., 2002; Boteler & Trichtchenko, 2015), and railways (Darch et al., 2014).

One example of space weather causing railway signaling issues occurred in Sweden during a geomagnetic storm in July 1982. A signal changed from green to red and back to green even though no train was present on the track or any other fault conditions existed. It was later estimated that the storm induced a geoelectric field of 4-5 V/km (Wik et al., 2009), and the malfunction was explained by GICs flowing through the railway signaling network. Statistical analyses to explore the possible correlation between railway infrastructure misoperations and geomagnetic disturbances revealed a rise in the number of unexplained signal misoperations during periods of high geomagnetic activity, showing links between operational anomalies in railway infrastructure and geomagnetic interference (Kasinskii et al., 2007; Ptitsyna et al., 2008; Eroshenko et al., 2010).

In 2012, severe space weather was added to the UK National Risk Register of Civil Emergencies (Cabinet Office, 2012). Following this, the Department for Transport com-

missioned a report on the impact of space weather on UK railway infrastructure. This report identified knowledge gaps related to track circuit interference, noting that railway assets, including signaling systems, are potentially vulnerable to the effects of space weather (Darch et al., 2014). To further explore the impacts of space weather on railways and raise awareness among network operators, the European Commission's Joint Research Centre, the Swedish Civil Contingencies Agency, the UK Department for Transport, and the US National Oceanic and Atmospheric Administration jointly organized the "Space Weather and Rail" workshop in 2015, highlighting similar knowledge gaps in this area of study (Krausmann et al., 2015).

Patterson et al. (2023) (from here on referred to as P23) conducted an initial investigation of how DC track circuit signaling systems on AC electrified railways in the United Kingdom are impacted by GICs. The study focused on the simplest case of misoperation, known as "right side" failures, where the energized relay in a block with no train present is de-energized by GICs. The analysis involved building a network model of two UK railway lines (detailed in Section 3 below) and applying varying levels of uniform geoelectric field to identify the thresholds for "right side" failure. The study concluded that the return period for an event strong enough to cause "right side" failures would be about once every 30 years, and that a 1-in-100 year event would cause a significant number of misoperations across both lines. The model was built upon earlier work by Alm (1956), Lejdström and Svensson (1956), and Boteler (2021). In this paper, we extend the work described above to focus on the potentially hazardous failure mode, known as "wrong side" failures, which occur when a de-energized relay in a block with a train present is re-energized, making the block seem clear when it is occupied.

Section 2 details the operational principles of track circuit signaling and describes how misoperations may occur. Section 3 provides some background for the model in this study and the modifications made to produce this newest iteration. In Section 4, we provide the results of the modeling. In 4.1 and 4.2, we show the effects of the additions to the model (cross bonds and train axles, respectively) and how they may impact the results; 4.3 gives the threshold electric fields for "wrong side" failures, and 4.4 discusses how those thresholds differ with changes to the leakage to the ground due to weather conditions. Section 4.5 shows the resultant currents through the relays at a range of electric field values from the misoperation threshold to a 1-in-100 year extreme.

2 Track Circuit Signaling

A common system used to detect the presence of trains on railway line is the track circuit. Figure 1 shows the diagram for the case of an electrified railway line, insulated rail joints (IRJs) on one rail (the signaling rail) divide it into blocks, while the other rail (the traction rail) remains unbroken to act as a return path for the traction current that powers the train. At the beginning of each block is a relay, which is powered by a power supply at the other end of the block, with the current traveling through the signaling and traction rails. If there is no train present, the current energises the relay and a green signal is displayed, as in (a). However, if a train occupies the block, the current is redirected by the wheels and axle, preventing the relay from energizing and leading to a red signal, as in (b). To operate correctly, the relay requires the current to pass specific thresholds to energise or de-energise. However, this operation can be disrupted by GICs, which can cause "right side" failures or "wrong side" failures. On non-electrified railway lines, IRJs are commonly placed in both rails at the same positions. This means that the potential for misoperation due to space weather is lower, as there is equal induction in both rails, meaning no potential difference across the relay (Boteler, 2021).

As the speed of trains has increased over time, the basic, two-aspect, red/green signals have been substituted, where needed, for three-aspect or four-aspect signalling, which give drivers advanced notice of the signal state in the next three or four blocks. This al-
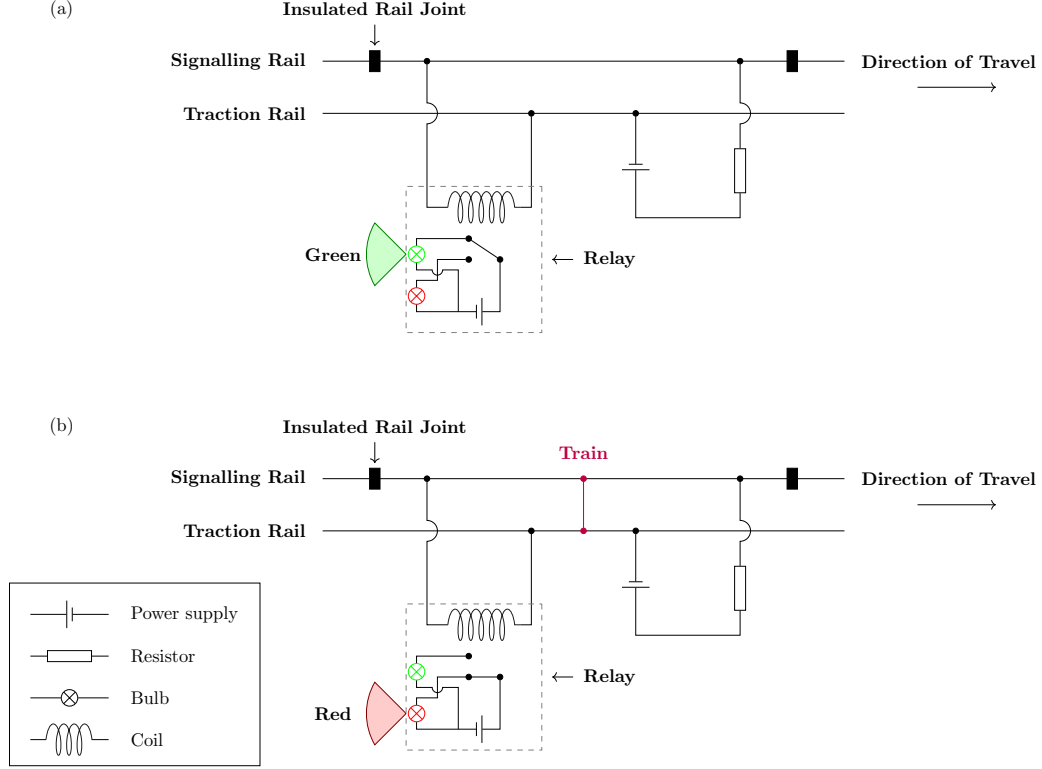
Figure 1. This circuit diagram shows a railway signaling track circuit for a single block within a network. The blocks are separated by insulated rail joints in the signaling rail, while the traction rail remains continuous. On the left side of the circuit (where the train enters from), a relay consisting of resistors and an electromagnet is connected. The power supply is situated on the right side of the block (where the train exits), accompanied by a resistor to protect it when train axles bypass the relay. In the absence of a train, (a), the relay is energized by the power supply, causing the signal to display a green light, indicating a clear section. However, when a train occupies the block, (b), the wheels and axle cut off the current from the power supply, de-energizing the electromagnet and causing the signal to display a red light, indicating an occupied section.
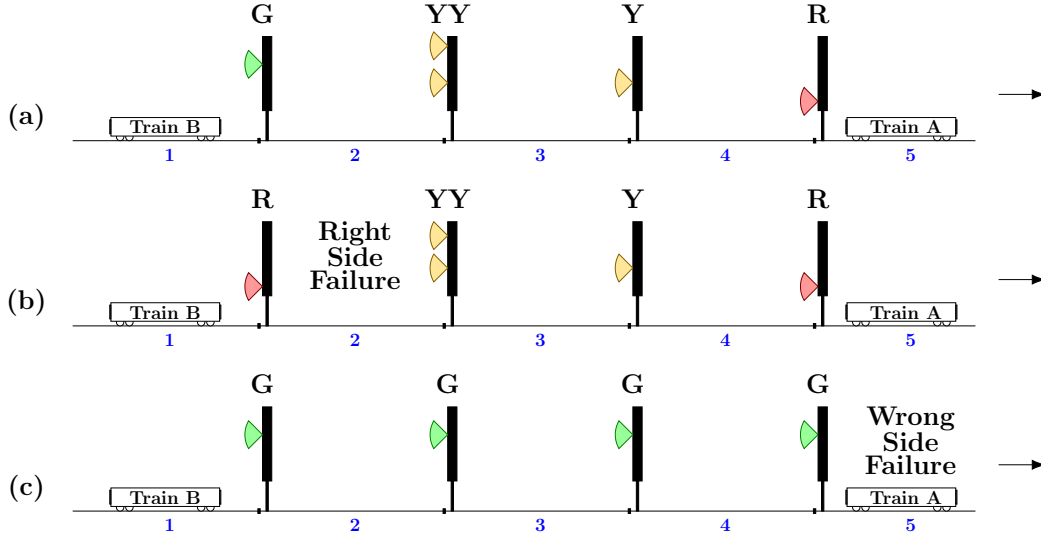
Figure 2. Diagram showing the operation of four-aspect signaling during (a) normal conditions, (b) a "right side" failure in block 2, and (c) a "wrong side" failure in block 5. The direction of travel is left to right.

lows them to have sufficient time to safely reduce their speed as they approach a red signal. Figure 2 demonstrates the principles of four-aspect signalling systems, and how "right side" and "wrong side" failures can impact their operation. In (a), we see normal operation: train A is occupying block 5, the four signals preceding it, from closest to furthest are red (danger/stop) - indicating there is a train occupying the next block, single yellow (caution) - indicating to the driver that they must stop at the next signal, double yellow (preliminary caution) - indicating that the next signal is a single yellow, and green (clear) - the train can proceed normally. If train A remains in block 5, train B would enter block 2 normally, start to slow down in block 3, and slow to a stop in block 4. In (b), a "right side" failure has occurred in block 2: without advanced caution from the single or double yellow signals, the driver of train B now sees the signal change from green to red, meaning they would have to decelerate the train more rapidly than normal to attempt to avoid passing the red signal. In the case of a space weather induced misoperation, there is nothing hazardous in block 2 causing the signal to change, it is the induced currents causing the relay to display the wrong signal. However, the driver does not know this, and the rapid deceleration of the train also has the potential to cause injuries to those on-board. In (c), a "wrong side" failure has occurred in block 5, currently occupied by train A: the driver of train B continues along the line, unaware that block 5 is actually occupied. This is potentially a far more hazardous case, as if the misoperation persists, there is the potential of a collision as the train B may not be able to decelerate fast enough to avoid colliding with the rear of train A. Three-aspect signalling uses the same principles described above, but without the double yellow signal.

In this study, the analyses focus on the Glasgow to Edinburgh via Falkirk line, however results are also given for the Preston to Lancaster section of the West Coast Main Line (WCML). Both lines were modeled in P23, and Glasgow to Edinburgh has been highlighted due to it being the more susceptible of the two, and because the entire line from start to finish is included in the model rather than a section of a longer line, as is the case with Preston to Lancaster. The Glasgow to Edinburgh line is split into 70 blocks with lengths varying between $0.4 - 1.9$ km, and the traction rail was calculated to be just over 76 km long. The Preston to Lancaster section of the WCML consists of 25 blocks

with lengths varying between $0.8 - 1.6\,\mathrm{km}$, and the traction rail was calculated to be just under $34\,\mathrm{km}$ long. It is also worth noting that Glasgow to Edinburgh line is predominantly east-west orientated, while Preston to Lancaster is largely north-south orientated.

3 Signaling System Modeling

The model used in this study is described in detail in P23. A summary of the modeling techniques is given forthwith, alongside details of additions made to the model to better represent a realistic railway signaling system and enable the analysis of "wrong side" failures.

The model considers each rail as a transmission line, composed of series impedances and parallel admittances. These elements represent the rail resistance and leakages to the ground, respectively. To simplify the model, the transmission line for each rail section is converted into an equivalent-pi circuit, consisting of current sources and admittances. The resulting circuits for both rails are combined with track circuit relay components to create a nodal admittance network (Boteler, 2021) as shown in Figure 3. The model parameters were sourced from Network Rail standards documents, ensuring their relevance to the UK case (see P23 for details).

3.1 Cross Bonding

Where previously the model considered only a single track (pair of rails) in one direction of travel, now it has been modified to include both directions of track, connected by wires of $1000\,\mathrm{S}$ ($1\,\mathrm{m\Omega}$) (NR/SP/SIG/50004, 2006) called cross bonds which electrically bond both traction rails every $400\,\mathrm{m}$ (NR/SP/ELP/21085, 2007). The main purpose of cross bonds is to ensure traction rail continuity, if there is a break in one of the traction rails, the traction return current still has an alternate path to flow.

3.2 Train Axles

To study "wrong side" failures, the admittances of train axles that connect the signaling and traction rails must be considered. The Glasgow to Edinburgh via Falkirk line mainly uses British Rail Class 385 AT-200 trains built by Hitachi Rail for ScotRail. We have used the three-car set as an example, but the model could easily be adapted to other train configurations. Every car has four wheelsets (two at each end) each consisting of two wheels and an axle, and the distances between the axles has been estimated based on specifications given by Iwasaki et al. (2017), and shown in Figure 4. It is assumed that each axle has a resistance (known as the train shunt resistance) of $25.1\,\mathrm{m\Omega}$ ($39.8\,\mathrm{S}$) (NR/SP/SIG/50004, 2006). For Preston to Lancaster, we have used the 11-car British Rail Class 390 Pendolino trains, assuming each car has the same axle dimensions as the Class 385 given above.

4 Results

4.1 Cross Bonding Effects

To study the effects that cross bonds have on the current through the relays at different magnitudes of geoelectric field strength, we have run the model both with and without the inclusion of cross bonds for 0, 5, and $-5\,\mathrm{V\,km^{-1}}$ and compared the results. Figure 5 shows the current differences through the relays when cross bonds are added. For each relay in the eastwards direction, we see that the current differences are shifted in a positive or negative direction depending on the orientation of the electric field, and this shift is reversed for the opposite direction of travel. We also see that the extent to which the current differences change with electric field strength is less prominent at the ends of the line and more significant at the centre. This is due to the inherent properties of the line shown in P23, and the shorter length of track circuit blocks at both ends of the
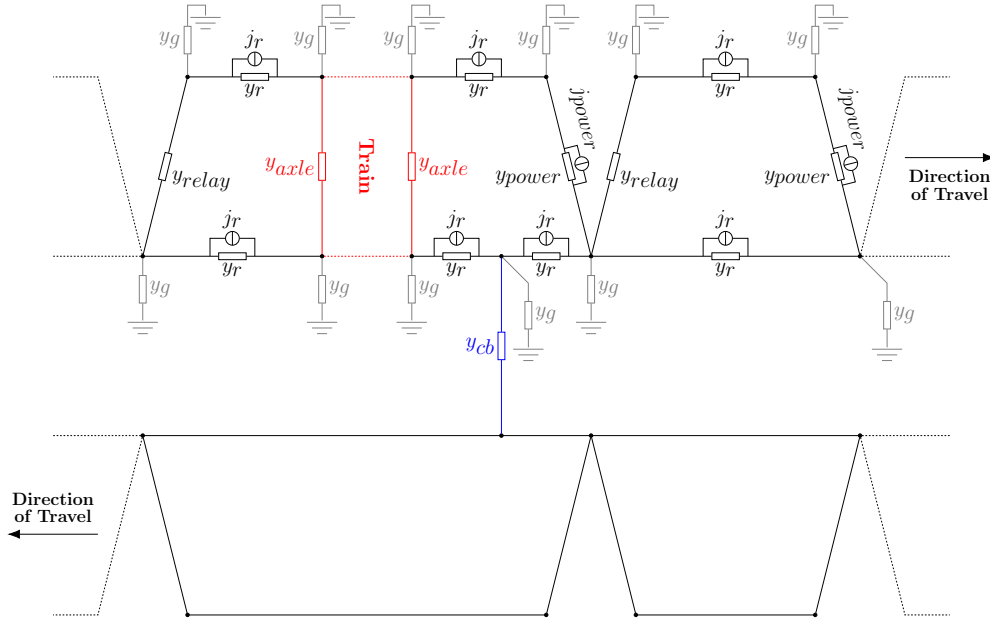
Figure 3. Circuit diagram showing the nodal admittance network of a section of a line with two track circuit blocks in each direction of travel. Track circuits are separated by insulated rail joints but share a continuous traction rail. The traction rails are periodically connected with cross bonds (shown in blue), and there is a train in top left block (shown in red). Only the first and last axle of the train is shown here for simplification, but every axle is included in the model. The components making up the network are the current source and admittance of the power supply (j_{power} and y_{power} respectively), the admittance of the relay (y_{relay}), the admittance to the ground at each node (y_g), the admittance due to the rail between nodes, (y_r), the currents induced in the rails due to the geoelectric field between nodes (j_r), the admittance of the cross bond (y_{cb}), and the admittance of the train axles (y_{axle}). The bottom track has been simplified for legibility.
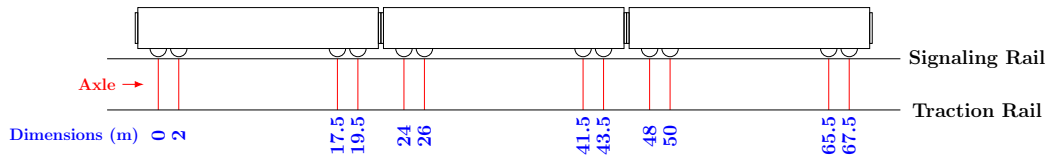

Figure 4. The dimensions of the wheelsets for the three-car British Rail Class 385 AT-200 that is used on the Glasgow to Edinburgh via Falkirk line. The axles (shown in red) electrically connect both rails, as the current travels between the rails through the wheels and axle.
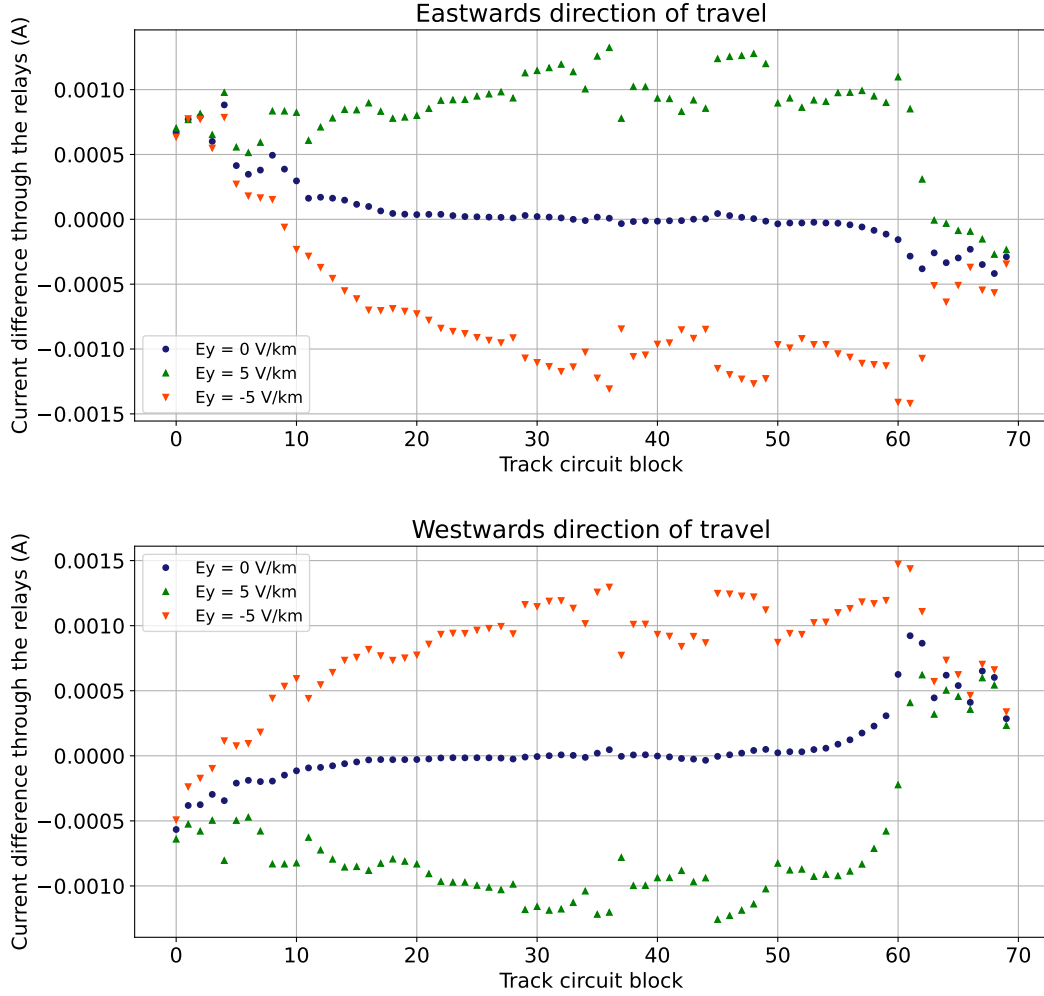
Figure 5. The difference in current through the relays on the Glasgow to Edinburgh via Falkirk line when cross bonds are added for the eastwards and westwards direction of travel at electric field values of 0, 5, and $-5\,\mathrm{V\,km^{-1}}$. The current differences are shifted in a positive or negative direction depending on the orientation of the electric field, and this shift is reversed for the opposite direction of travel.

line, which may not contain a cross bond. When compared with the range of normal current values of -0.5 to $0.5\,\mathrm{A}$, it is apparent that the magnitude of the current differences is very small, so the inclusion of cross bonds has minimal impact on the operation of the track circuits both during normal operation and during a geomagnetic storm.

4.2 Distance Along a Block

While investigating the conditions required for "wrong side" failures to occur, it was found that the position of the train in a block is a major factor, as the distance a train has travelled along the block, and hence the lengths of rail between the rear-most axle and the start of the block, will impact the amount of GIC that can affect the relay.
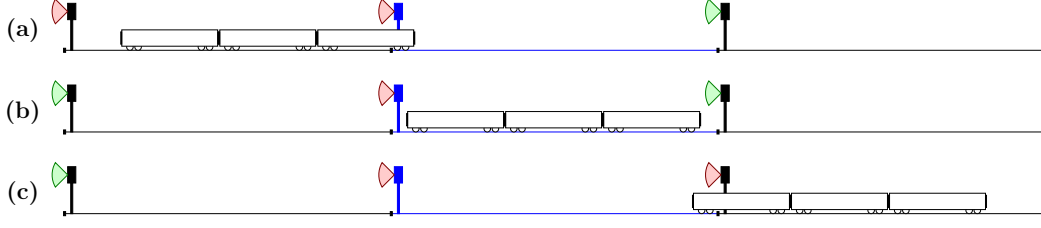
Figure 6. Diagram showing how the signals in a two-aspect system change as a train is travelling along a line. In (a), the train has just entered the block, the signal changes to red as the axles bypass the relay. The signal in the previous block remains red, as it is still occupied by the back end of the train. In (b), the train is now completely within a block, the signal in the previous block changes to green as it is now unoccupied. In (c), almost the entire train has entered the next section, turning the signal for that block red. When the train is positioned at this end of the block, the potential for "wrong side" failure is highest, as it is the maximum distance between the relay and the axles of the train while the train is still occupying the block.

Assuming two-aspect signalling for simplification, Figure 6 shows how the signals change as a train moves along the line. Focusing on the middle (blue) block: In (a), when a train first enters the block, the signal changes to red as the axles bypass the relay. At this point, the signal in the previous block should also be red, as the train has yet to vacate it completely. In (b), the train has moved forward such that it is now completely within the block, the signal behind changes to green as the previous block is now unoccupied. As the train starts moving away from the relay, if there is an external electric field, induction in the rails behind the train starts to drive a current through the relay. Figure 7 shows that because the relay is positioned at the end of the block that the train enters from, the length of rail on the relay side of the train (from which induced currents can reach the relay) increases as the train moves through the block, causing the amount of induced current through the relay to increase as the train progresses. The effect on the current through the relay is shown in Figure 8, where we see the magnitude of the current increases with both distance travelled through the block and the electric field strength applied. Finally, in (c), most the train has passed into the next block, turning the signal for that section red. When the train is in this position, the potential for "wrong side" failure is highest, as it is the maximum distance between the relay and the axles of the train while the train is still occupying the block. It is also worth noting that the unoccupied blocks (with green signals) are potentially vulnerable to misoperations in the form of "right side" failures. In the analyses below, the positions of the trains are always set at the power supply end of the block, i.e., just prior to exiting the block, to model the worst case scenario in terms of positioning that will have the biggest impact on signaling systems.

4.3 Thresholds for "Wrong Side" Failure

To find the thresholds at which "wrong side" failures occur for each block in both directions of travel, uniform electric field values were applied to each block (eastwards orientated for Glasgow to Edinburgh and northwards orientated for Preston to Lancaster) until the first "wrong side" failure occurred, and the electric field strength at that point was recorded. In this case, the train is at the power supply end of the block to allow the largest amount of induced current to reach the relay. Figure 9 shows the threshold electric field required to trigger a "wrong side" failure in each track circuit block for both directions of travel on the Glasgow to Edinburgh line. The blue crosses indicate the threshold at standard leakage values, while the blue lines illustrate how the threshold changes
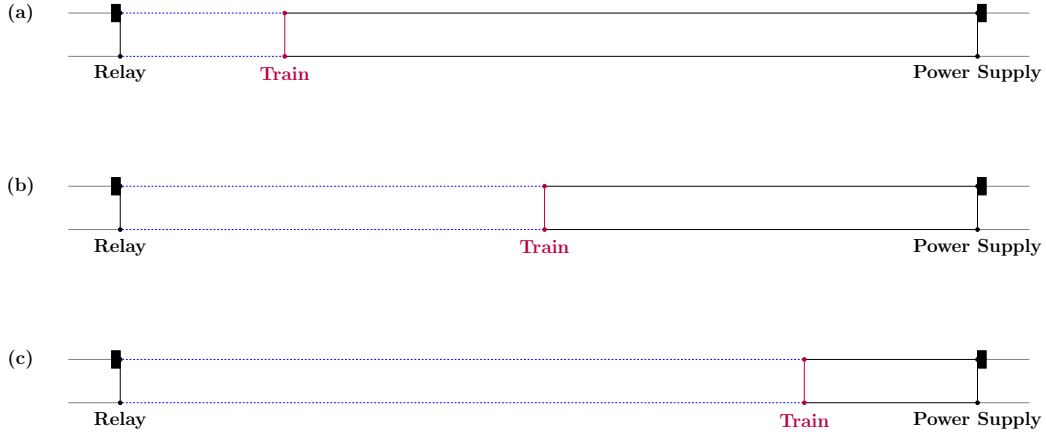
Figure 7. Train axles (indicated by vertical purple lines) cut off the power supply current from the relay, effectively splitting the block into two circuits. The number of axles on a train is dependent on the number of carriages, only a single set is shown here for simplicity. In this case, the only source of current reaching the relay is induced in the rails by the electric field. The blue (dashed lines) show the portion of the rails within the relay-side circuit, as the train moves from its position in (a) to (b) to (c), the size of the relay-side circuit grows, and more of the current induced in the rails can reach the relay.
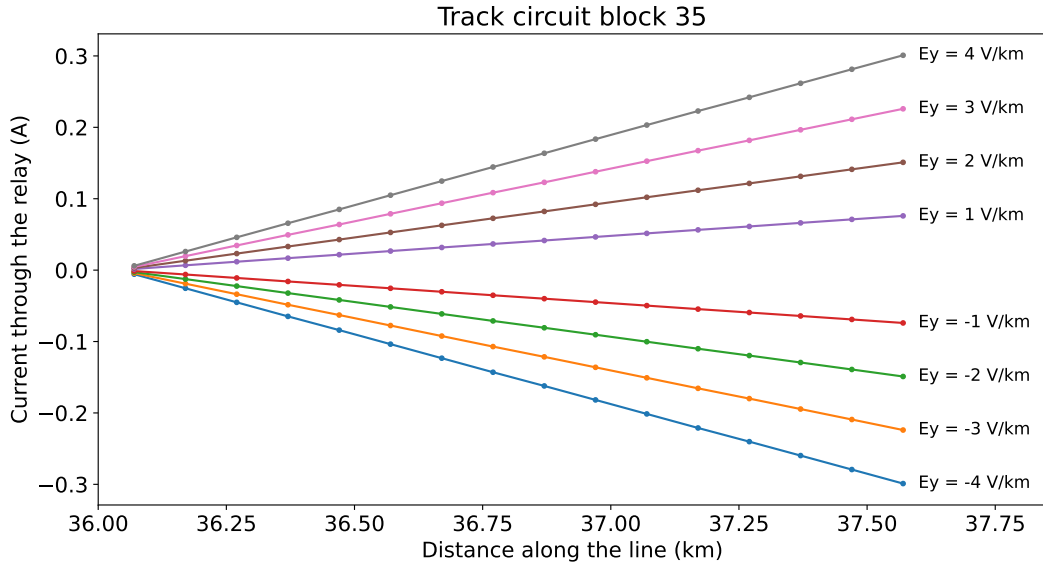

Figure 8. As a train passes through a track circuit block, the magnitude of current across the relay increases. This is due to the distance along the block between the axle (which is cutting off the power supply current) and the relay increasing, so more of the rail's induced current is able to reach the relay. The magnitude of the current through the relay also increases with an increased electric field strength.
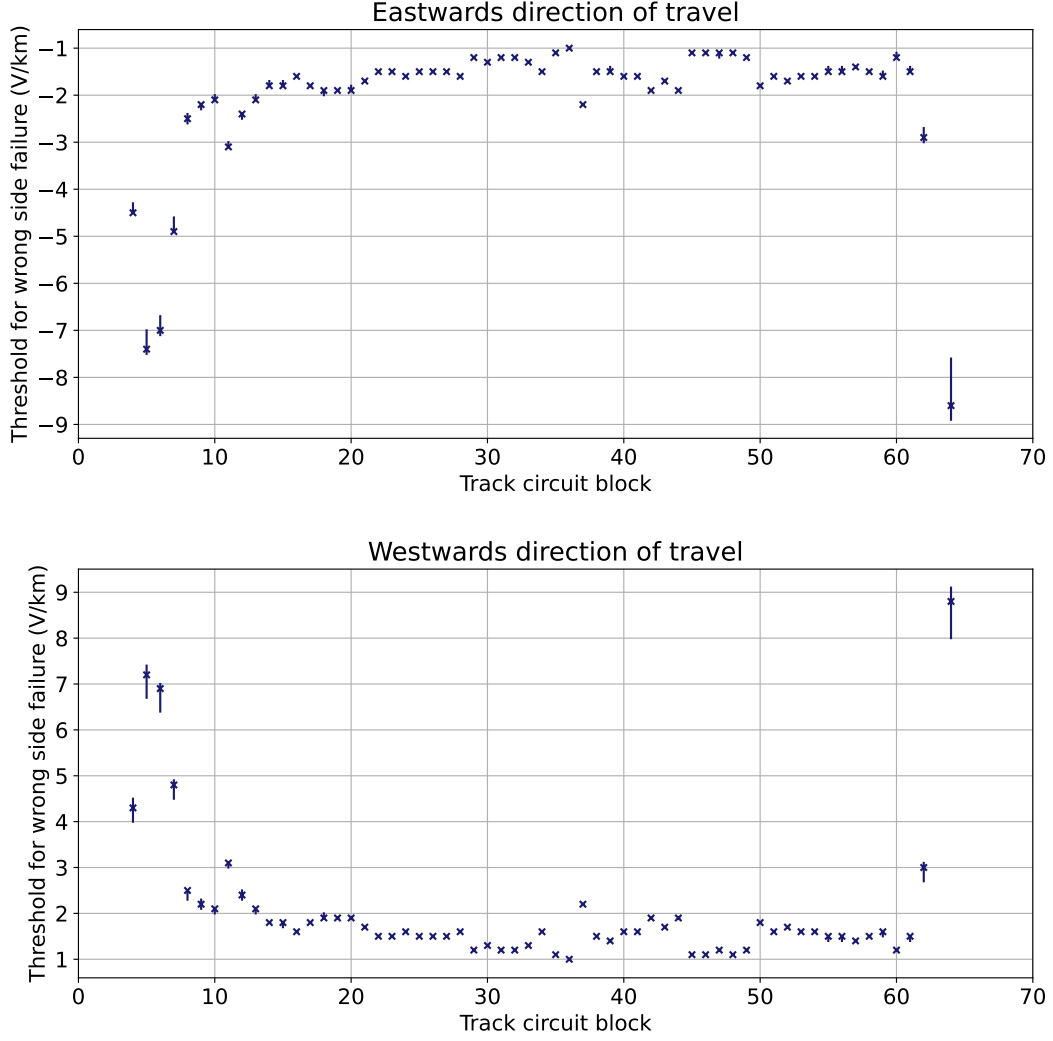
Figure 9. Glasgow to Edinburgh: The threshold electric field values to cause "wrong side" failure for each track circuit block in both eastwards and westwards directions of travel. The blue crosses indicate the threshold at a standard leakage value, with the blue lines indicating how this threshold may differ with changes in leakage due to environmental conditions. We can see that the most susceptible track circuit block is number 36 for both the eastwards and westwards with threshold values of $-1\,\mathrm{V\,km^{-1}}$ and $1\,\mathrm{V\,km^{-1}}$ respectively.

with differing leakage in response to environmental conditions, as described in section 4.4. Minimum and maximum values leakage values are given in P23. It is shown that the minimum threshold for "wrong side" failure occurs in track circuit block 36 for both the eastwards and westwards directions of travel with values of $-1\,\mathrm{V\,km^{-1}}$ and $1\,\mathrm{V\,km^{-1}}$ respectively. This is likely due to its position towards the centre of the line, its long block length, and its almost horizontal orientation. Figure 10 shows the results for Preston to Lancaster, the minimum threshold for "wrong side" failure occurs in track circuit block 6 for northwards and southwards directions of travel with values of $-1.1\,\mathrm{V\,km^{-1}}$ and $1.1\,\mathrm{V\,km^{-1}}$ respectively.

As the magnitude of the electric field is increased, the number of "wrong side" failures increases. This relationship is shown for the Glasgow to Edinburgh line in Figure
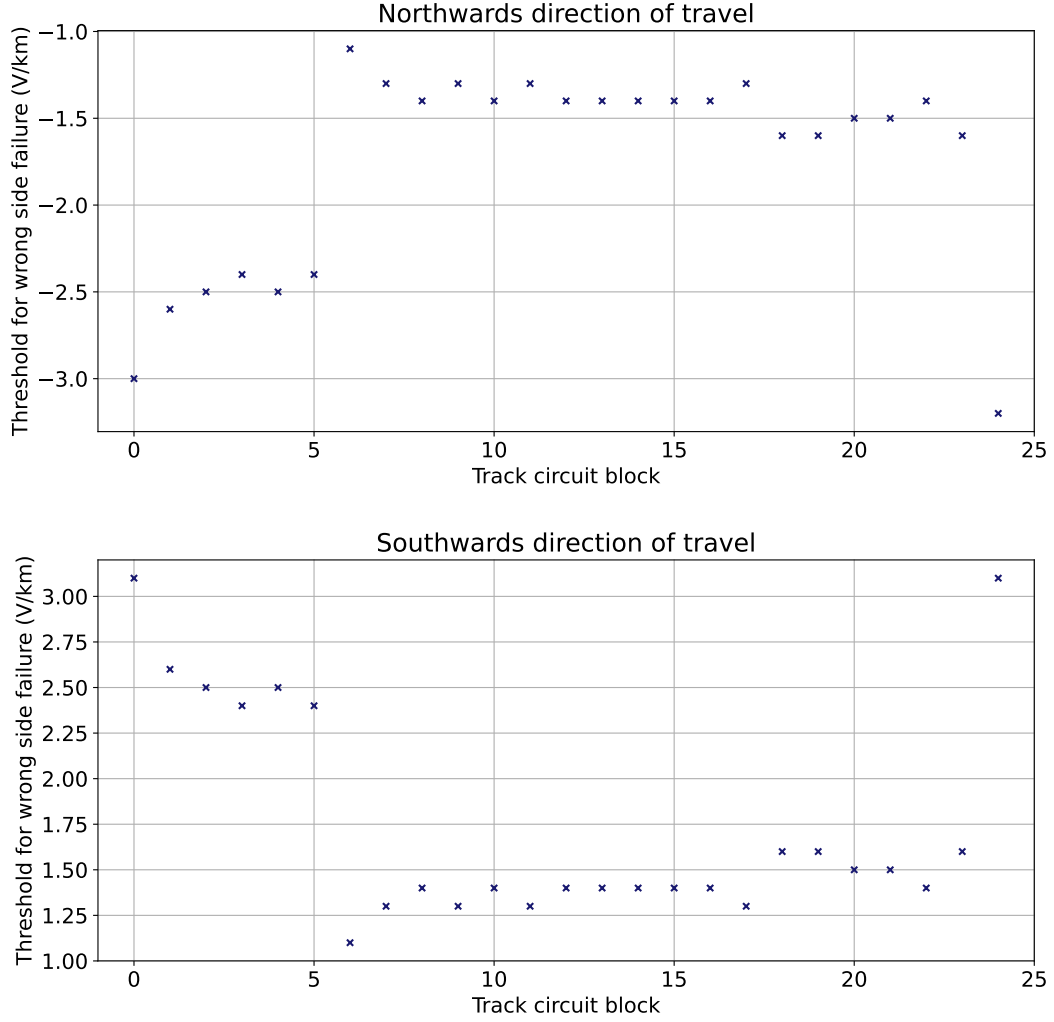
Figure 10. Preston to Lancaster: The threshold electric field values to cause "wrong side" failure for each track circuit block in both northwards and southwards directions of travel. The blue crosses indicate the threshold at a standard leakage value. We can see that the most susceptible track circuit block is number 6 for northwards and southwards directions of travel with threshold values of $-1.1\,\mathrm{V\,km^{-1}}$ and $1.1\,\mathrm{V\,km^{-1}}$ respectively.
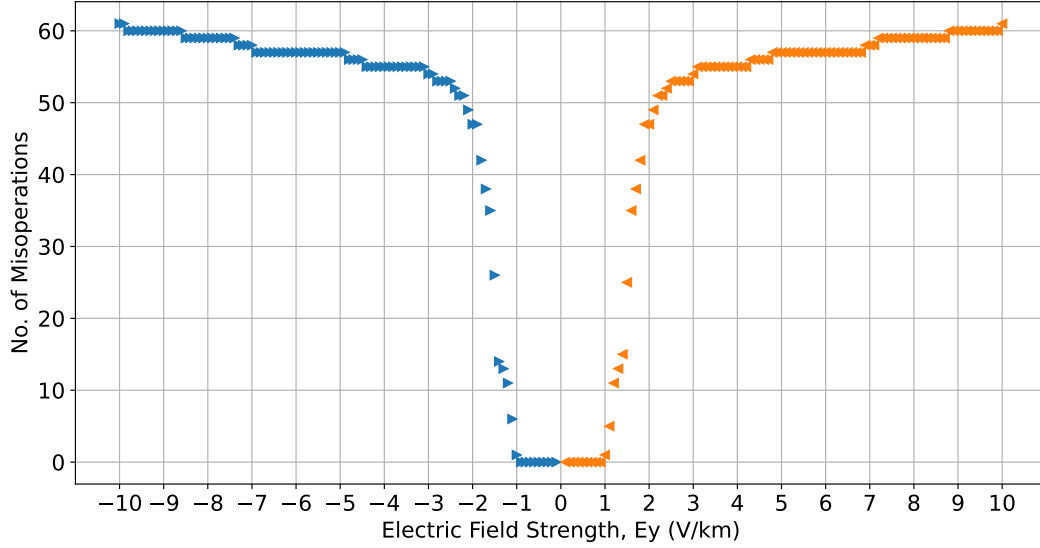
Figure 11. Glasgow to Edinburgh: The number of track circuit blocks with the potential to experience "wrong side" failures at different magnitudes of electric field strength for both the eastwards and westwards directions of travel. The blue (right facing) triangles and the orange (left facing) triangles indicate the eastwards and westwards directions of travel respectively.

11. The blue (right facing) triangles indicate the eastwards direction of travel and the orange (left facing) triangles are the westwards direction of travel. Between 1 to $3\,\mathrm{V\,km^{-1}}$ for the westwards direction of travel and -1 to $-3\,\mathrm{V\,km^{-1}}$ for the eastwards direction of travel, there is a steep increase in the number of "wrong side" failures, meaning that the threshold for misoperation for most blocks lies within these ranges. Beyond $\pm3\,\mathrm{V\,km^{-1}}$, larger increase in the magnitude of the electric field strength is needed to cause further "wrong side" failures. This is due to multiple factors: (1) some blocks are orientated in such a way that the component of the eastwards electric field parallel to the rails is small, so a larger electric field is needed to induce enough current to cause a misoperation; (2) blocks of shorter length need larger electric fields to induce the currents required to cause a misoperation; (3) the innate properties of the transmission line discussed in P23, which are independent of block length and orientation, cause the current through the relays in blocks at the ends of each line to be more resistant to changes with electric field strength. These factors mean that the threshold for "wrong side" failure in some blocks is much higher, a few of which exceed hundreds of volts per kilometer and are not shown here. We see a similar result for Preston to Lancaster in Figure 10, however, as it is a centre section of the WCML, we do not see the effects of the ends of the line as we do in Glasgow to Edinburgh. At $-3.2\,\mathrm{V\,km^{-1}}$ and $3.1\,\mathrm{V\,km^{-1}}$ respectively, all of the relays in the northwards and southwards directions of travel would experience misoperations.

4.4 Effects of Leakage Change

The leakage from the rails to the ground can change with environmental conditions, increasing in wetter weather and decreasing in drier weather. The model was run with multiple leakage values derived from Network Rail standard NR/GN/ELP/27312 (2006) and given in P23 to provide a range of "wrong side" failure thresholds. Figure 9 shows that increasing or decreasing the leakage of the rails affects the track circuit blocks towards the ends of the line more than at the centre, this is largely due to the properties of the transmission line. This can be demonstrated by creating a test network of $70\times1\,\mathrm{km}$
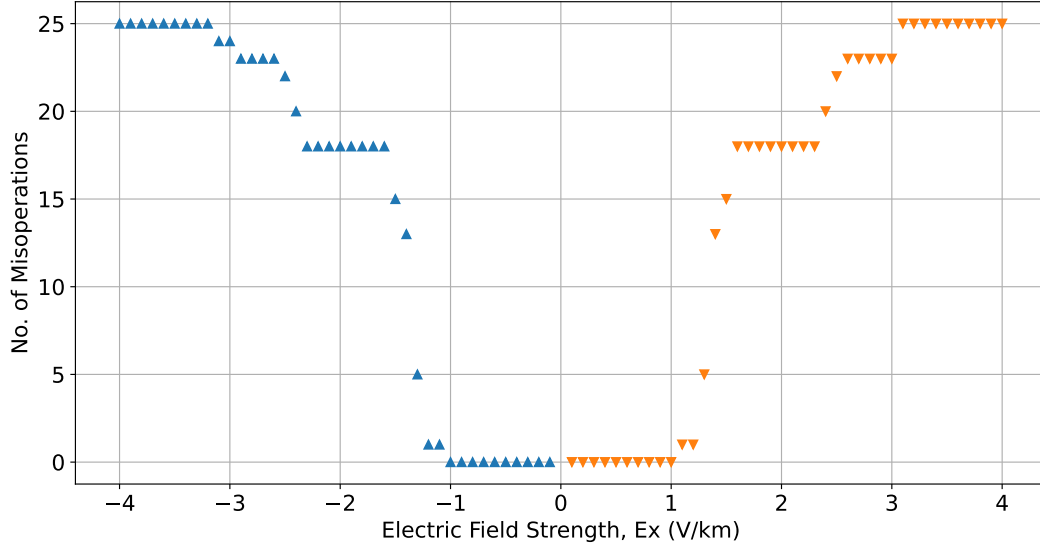
Figure 12. Preston to Lancaster: The number of track circuit blocks with the potential to experience "wrong side" failures at different magnitudes of electric field strength for both the northwards and southwards directions of travel. The blue (up facing) triangles and the orange (down facing) triangles indicate the northwards and southwards directions of travel respectively.

blocks in each direction of travel with the same orientation (parallel to the electric field direction), each occupied by a train. This makes the results independent of the two other main factors that determine the misoperation thresholds - block length and orientation. In Figure 13, the blue crosses indicate standard leakage, the orange (upwards) triangles are maximum leakage, and the green (downwards) triangles are minimum leakage. It is shown that the difference in leakage has a larger impact on the current through the relays that are near the ends of the line when compared with those in the middle, hence the threshold for "wrong side" failures for at blocks near the end are more sensitive to changes in leakage due to transmission line properties, and not block length or orientation. This explains why in Figure 10 we do not see leakage having an impact on the blocks in the Preston to Lancaster section of the WCML, due to it being a centre part of a longer line.

4.5 Applying Uniform Electric Fields

In the following analysis, we have used the example where 7 trains (5 for Preston to Lancaster) are relatively evenly spread along the line, this is so we can show "right side" failures occurring at the same time as "wrong side" failures. The choice of number of trains is arbitrary, as this is by no means a fixed case in reality, and can differ greatly depending on the density of traffic, which in turn changes depending on the time of day. The number of "wrong side" failures is dependent on how many trains are occupying the blocks and where those occupied blocks are along the line, so in the examples below, as well as showing the results for this setup, we will also use Figure 11 to provide a number of how many relays would be susceptible to "wrong side" failure if they were occupied.
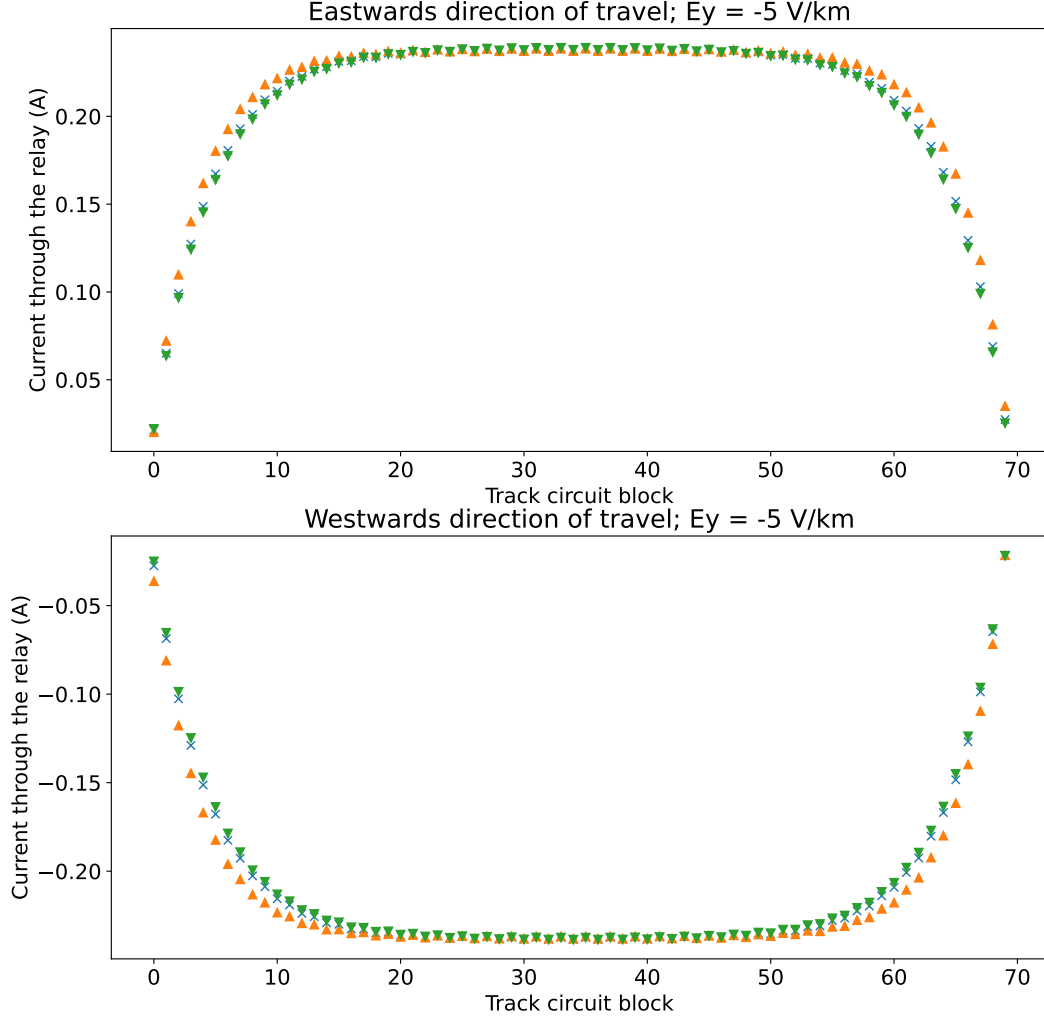
Figure 13. The current through the relays in the eastwards and westwards directions for the $70{\times}1$ km block test network where all blocks are orientated parallel to the direction of the electric field ($E_y = -5\,\mathrm{V\,km^{-1}}$). The blue crosses indicate standard leakage, the orange (upwards) triangles are maximum leakage, and the green (downwards) triangles are minimum leakage.

4.5.1 Threshold Value

Figure 14 (a) and (b) shows the current through the relay of each track circuit block in the eastwards and westwards directions of travel, respectively, assuming no external electric field is applied. The red (solid) line is the 'drop-out current' the value below which the current must drop to de-energise the relay, turning the signal red; the green (dashed) line is the 'pick-up current', the value above which the current must rise to energise the relay, turning the signal green. A green ring with no fill indicates an unoccupied block operating normally, and a red triangle with no fill is an occupied block operating normally, with the direction of the triangle showing the direction of travel (right for eastwards and left for westwards). It can be seen that under these conditions, all relays are operating normally. The threshold electric field value at which "wrong side" failures begin to occur is shown in the bottom two panels, $E_y = -1\,\mathrm{V\,km^{-1}}$ for eastwards (c), and $E_y = 1\,\mathrm{V\,km^{-1}}$ for westwards (d). In both directions of travel, block 36 experiences the first "wrong side" failure, which is indicated by a filled green triangle. Figure 15 shows the same results for Preston to Lancaster, with the direction of the triangle showing the direction of travel (right for northwards and left for southwards). The threshold electric field value at which "wrong side" failures begin are $E_x = -1.1\,\mathrm{V\,km^{-1}}$ for northwards (c), and $E_x = 1.1\,\mathrm{V\,km^{-1}}$ for westwards (d), occurring in block 6 in both cases.

4.5.2 Known Misoperation Value

The magnitude of the electric field known to have caused signaling misoperations in the past in Sweden is estimated to be around $4\,\mathrm{V\,km^{-1}}$ (Wik et al., 2009). With an electric field of this strength applied, Figure 16 shows us that, for the Glasgow to Edinburgh line, both types of misoperation ("wrong side" failures and "right side" failures) occur. The number of track circuits that could potentially experience a "wrong side" failure is 55 for both eastwards at $E_y = -4\,\mathrm{V\,km^{-1}}$ and westwards at $E_y = 4\,\mathrm{V\,km^{-1}}$. As for "right side" failures, we see 16 for eastwards at $E_y = 4\,\mathrm{V\,km^{-1}}$ and 12 for westwards at $E_y = -4\,\mathrm{V\,km^{-1}}$. Figure 17 shows the results for Preston to Lancaster, where the number of track circuits that could potentially experience a "wrong side" failure is 25 for both northwards at $E_x = -4\,\mathrm{V\,km^{-1}}$ and southwards at $E_x = 4\,\mathrm{V\,km^{-1}}$. As for "right side" failures, we see all 5 occupied blocks misoperating in both cases.

4.5.3 1-in-100 Year Extreme Estimate

If we apply the estimate for a 1-in-100 year extreme geoelectric field for the UK, estimated by Beggan et al. (2013) to be approximately $5\,\mathrm{V\,km^{-1}}$, the results are shown in Figure 18. The number of track circuits that could potentially experience a "wrong side" failure increases slightly from the from $\pm 4\,\mathrm{V\,km^{-1}}$ value to 56 for eastwards at $E_y = -4\,\mathrm{V\,km^{-1}}$ and 57 westwards at $E_y = 4\,\mathrm{V\,km^{-1}}$. This is due to the relays towards the ends of the line having much higher thresholds and most relays having already misoperated between ± 1 to $3\,\mathrm{V\,km^{-1}}$. We do see an increase in the number of "right side" failures, with over a third of unoccupied relays misoperating in both directions of travel. For Preston to Lancaster in Figure 19, the number of track circuits that could potentially experience a "wrong side" failure cannot increase any further, as the threshold misoperation value for each track circuit had already been reached for both directions of travel at $\pm 4\,\mathrm{V\,km^{-1}}$. However, we do see an increase in the number of "right side" failures occurring in both directions of travel, with nearly all relays experiencing misoperation. The results for "right side" failures agree with P23. It is apparent that a 1-in-100 year extreme event would result in a significant number of signal misoperations.
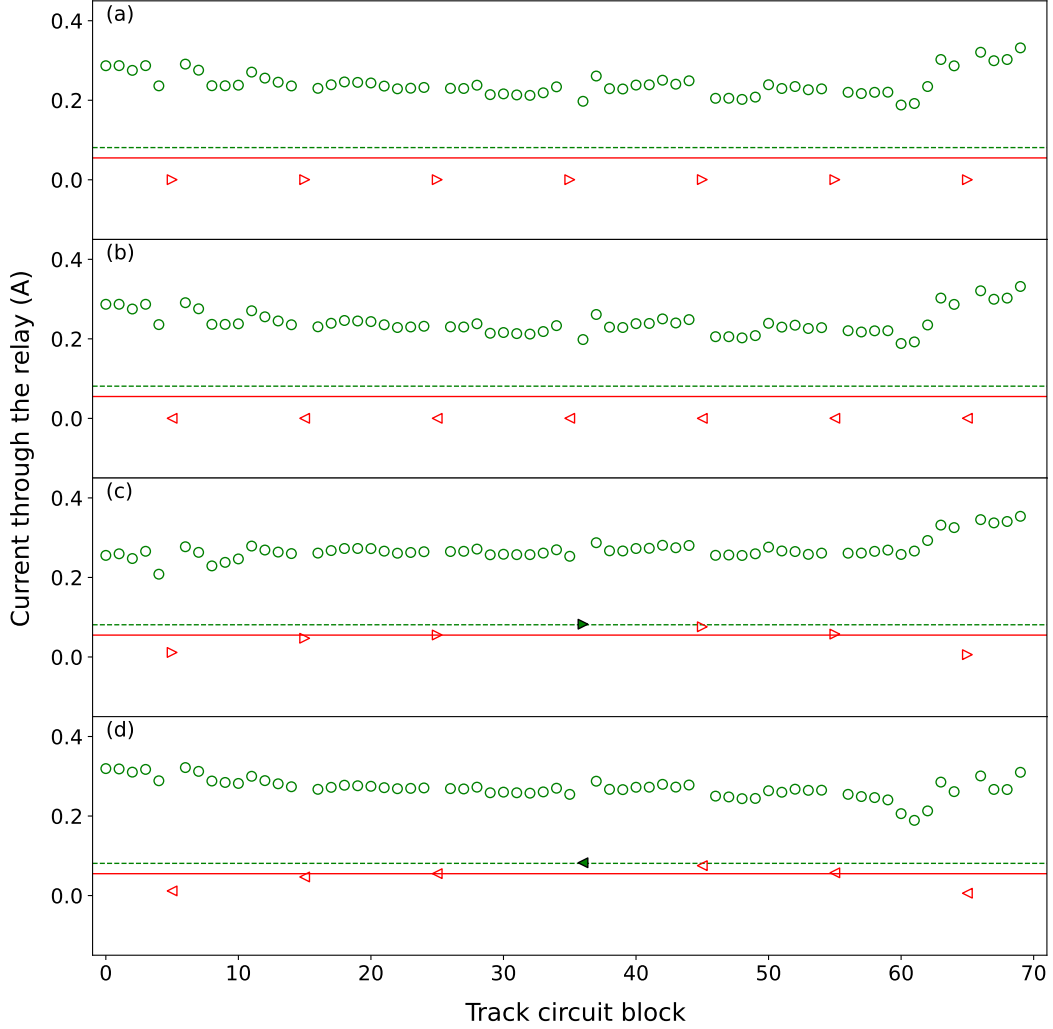
Figure 14. Glasgow to Edinburgh: The current through each relay when no electric field is applied for the eastwards (a) and westwards (b) directions of travel, and at the threshold for "wrong side" failure in the (c) eastwards and (d) westwards directions of travel. The red (solid) line is the 'drop-out current' the value below which the current must drop to de-energise the relay, turning the signal red; the green (dashed) line is the 'pick-up current', the value above which the current must rise to energise the relay, turning the signal green. A green ring with no fill indicates an unoccupied block operating normally, and a red triangle with no fill is an occupied block operating normally, with the direction of the triangle showing the direction of travel (right for eastwards and left for westwards). A filled green triangle indicated a "wrong side" failure. With no electric field applied, all relays are operating normally. At the threshold for "wrong side" failure, we see one misoperation in either direction of travel.
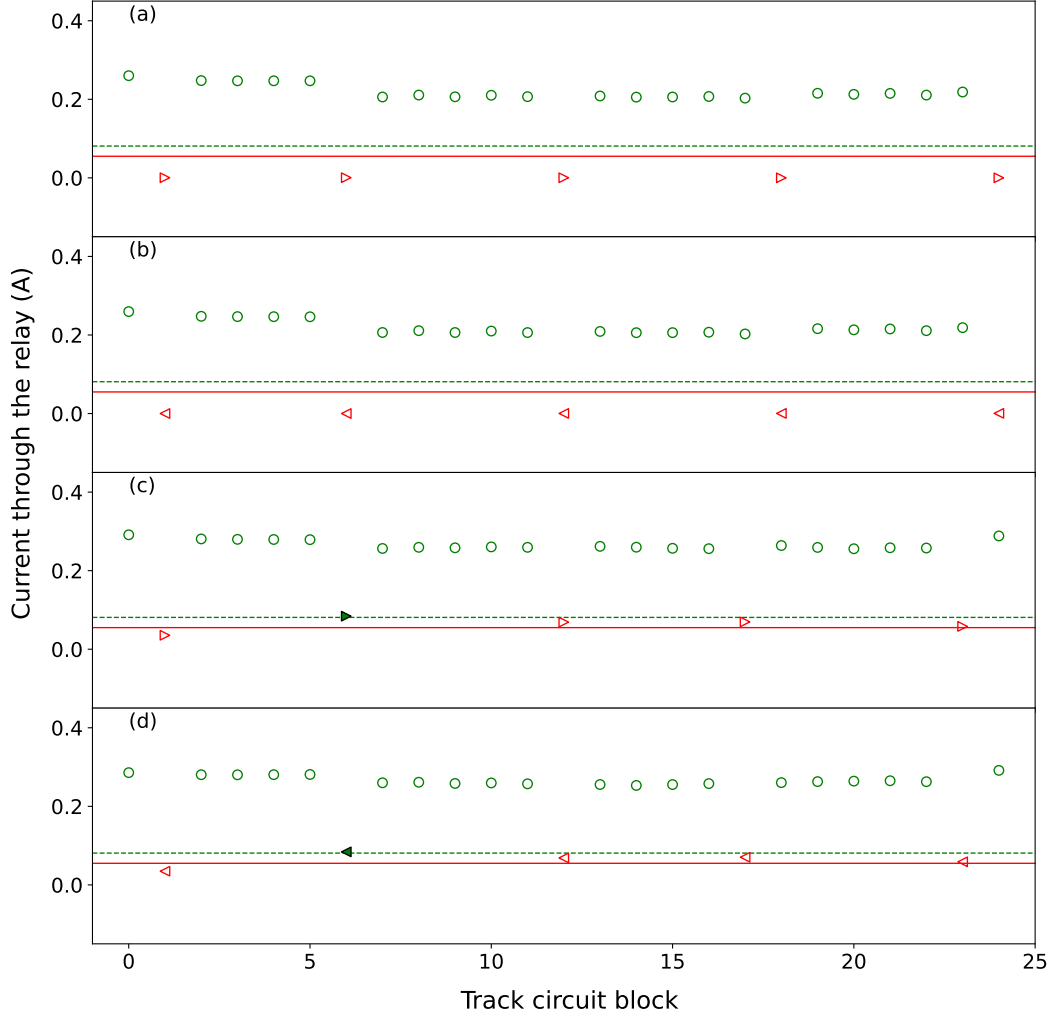
Figure 15. Preston to Lancaster: The current through each relay when no electric field is applied for the northwards (a) and southwards (b) directions of travel, and at the threshold for "wrong side" failure in the (c) northwards and (d) southwards directions of travel. The red (solid) line is the 'drop-out current' the value below which the current must drop to de-energise the relay, turning the signal red; the green (dashed) line is the 'pick-up current', the value above which the current must rise to energise the relay, turning the signal green. A green ring with no fill indicates an unoccupied block operating normally, and a red triangle with no fill is an occupied block operating normally, with the direction of the triangle showing the direction of travel (right for northwards and left for southwards). A filled green triangle indicated a "wrong side" failure. With no electric field applied, all relays are operating normally. At the threshold for "wrong side" failure, we see one misoperation in either direction of travel.
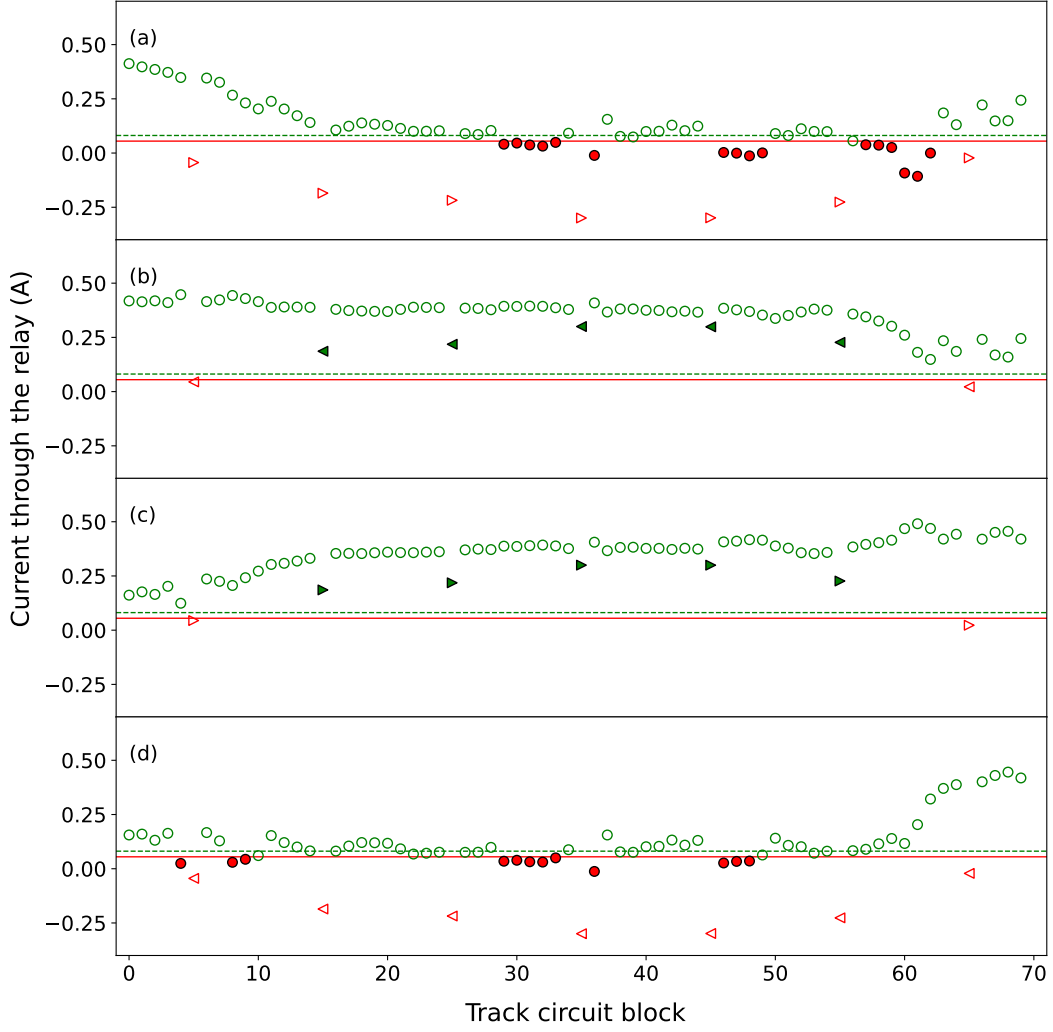
Figure 16. Glasgow to Edinburgh: The current through each relay at $E_y = 4\,\mathrm{V\,km^{-1}}$ in the (a) eastwards and (b) westwards directions of travel, and at $E_y = -4\,\mathrm{V\,km^{-1}}$ in (c) eastwards and (d) westwards directions of travel. The red (solid) line is the 'drop-out current' the value below which the current must drop to de-energise the relay, turning the signal red; the green (dashed) line is the 'pick-up current', the value above which the current must rise to energise the relay, turning the signal green. A green ring with no fill indicates an unoccupied block operating normally, and a red triangle with no fill is an occupied block operating normally, with the direction of the triangle showing the direction of travel (right for eastwards and left for westwards). A filled green triangle indicated a "wrong side" failure, and a filled red circle is a "right side" failure. Here we see both types of misoperation occurring in both directions depending on the orientation of the electric field.
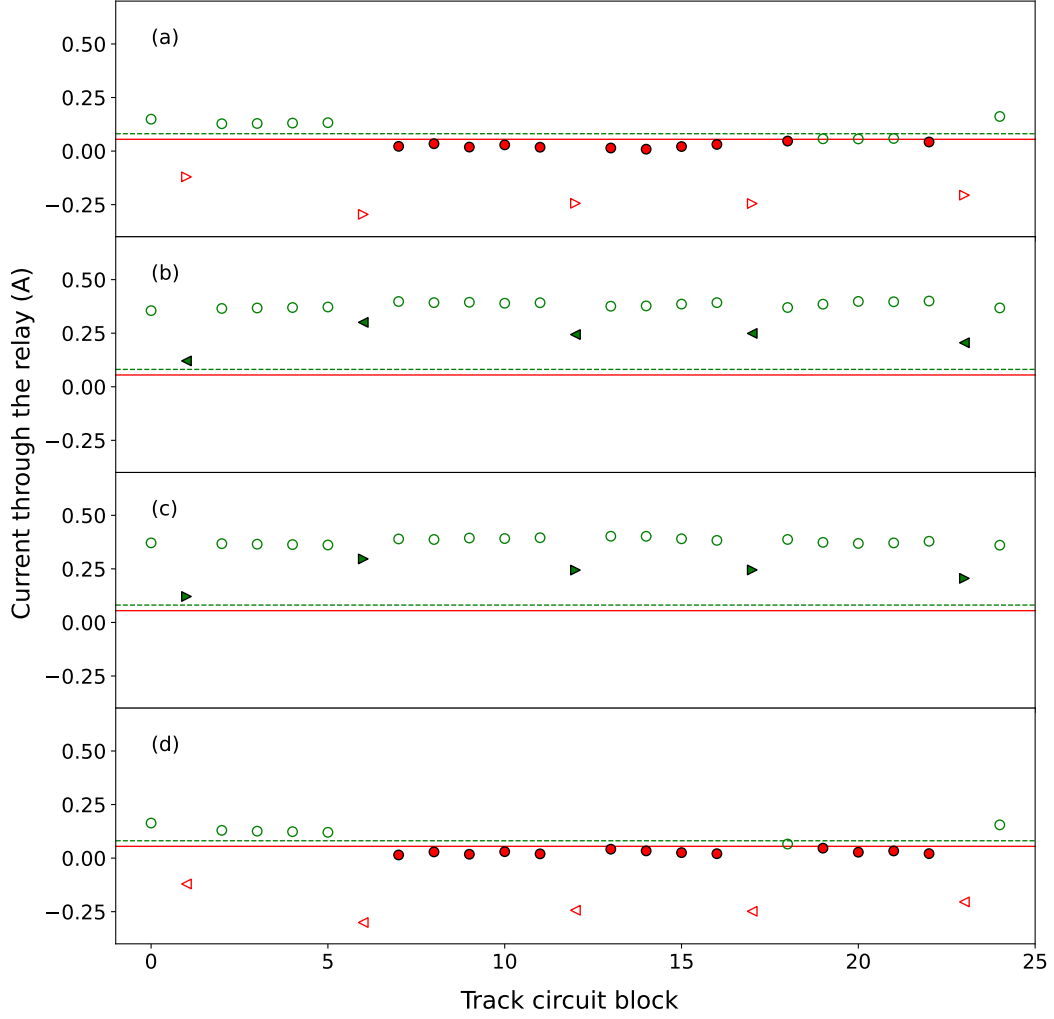
Figure 17. Preston to Lancaster: The current through each relay at $E_x = 4\,\mathrm{V\,km}^{-1}$ in the (a) northwards and (b) southwards directions of travel, and at $E_x = -4\,\mathrm{V\,km}^{-1}$ in (c) northwards and (d) southwards directions of travel. The red (solid) line is the 'drop-out current' the value below which the current must drop to de-energise the relay, turning the signal red; the green (dashed) line is the 'pick-up current', the value above which the current must rise to energise the relay, turning the signal green. A green ring with no fill indicates an unoccupied block operating normally, and a red triangle with no fill is an occupied block operating normally, with the direction of the triangle showing the direction of travel (right for northwards and left for southwards). A filled green triangle indicated a "wrong side" failure, and a filled red circle is a "right side" failure. Here we see both types of misoperation occurring in both directions depending on the orientation of the electric field.
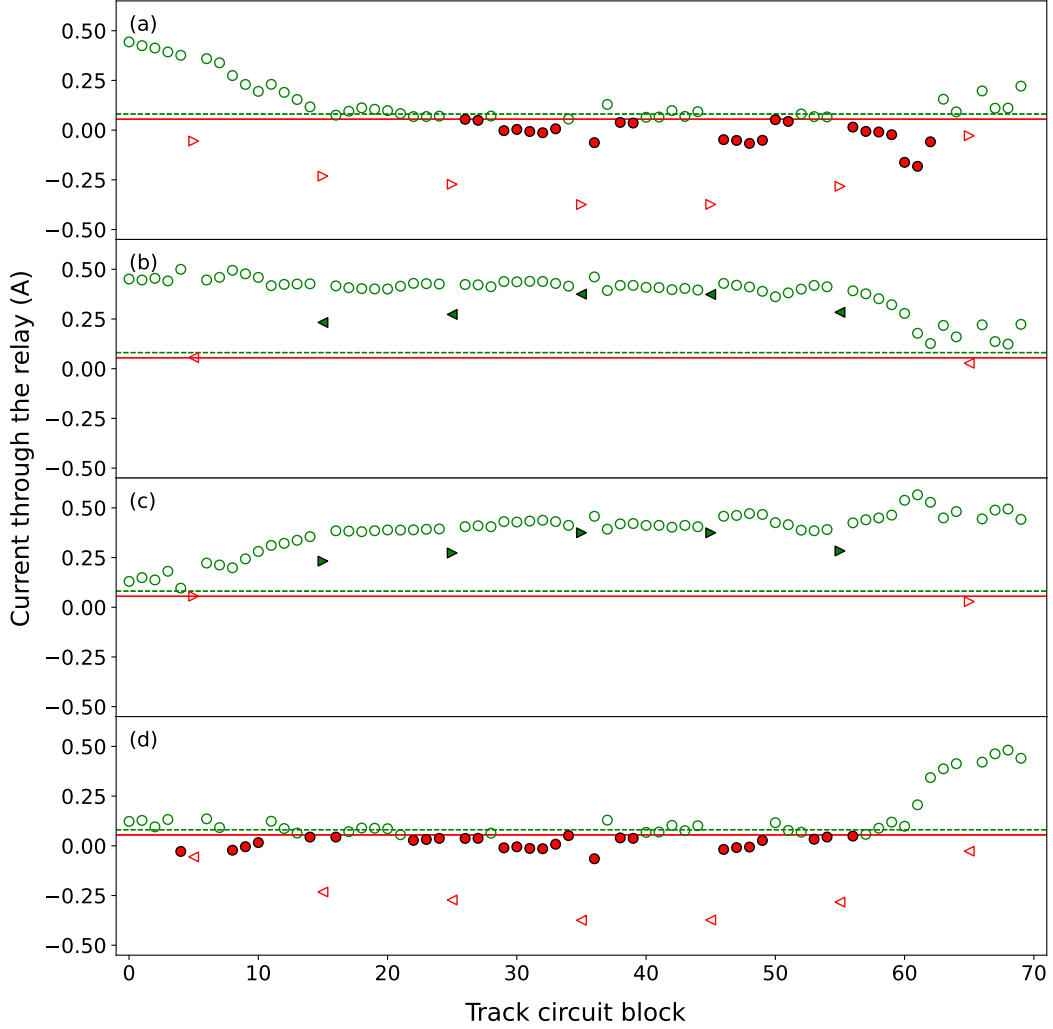
Figure 18. Glasgow to Edinburgh: The current through each relay at the 1-in-100 year extreme geoelectric field estimate of $E_y = 5\,\mathrm{V\,km^{-1}}$ in the (a) eastwards and (b) westwards directions of travel, and $E_y = -5\,\mathrm{V\,km^{-1}}$ in (c) eastwards and (d) westwards directions of travel. The red (solid) line is the 'drop-out current' the value below which the current must drop to de-energise the relay, turning the signal red; the green (dashed) line is the 'pick-up current', the value above which the current must rise to energise the relay, turning the signal green. A green ring with no fill indicates an unoccupied block operating normally, and a red triangle with no fill is an occupied block operating normally, with the direction of the triangle showing the direction of travel (right for eastwards and left for westwards). A filled green triangle indicated a "wrong side" failure, and a filled red circle is a "right side" failure. Here we see both types of misoperation occurring in both directions depending on the orientation of the electric field.
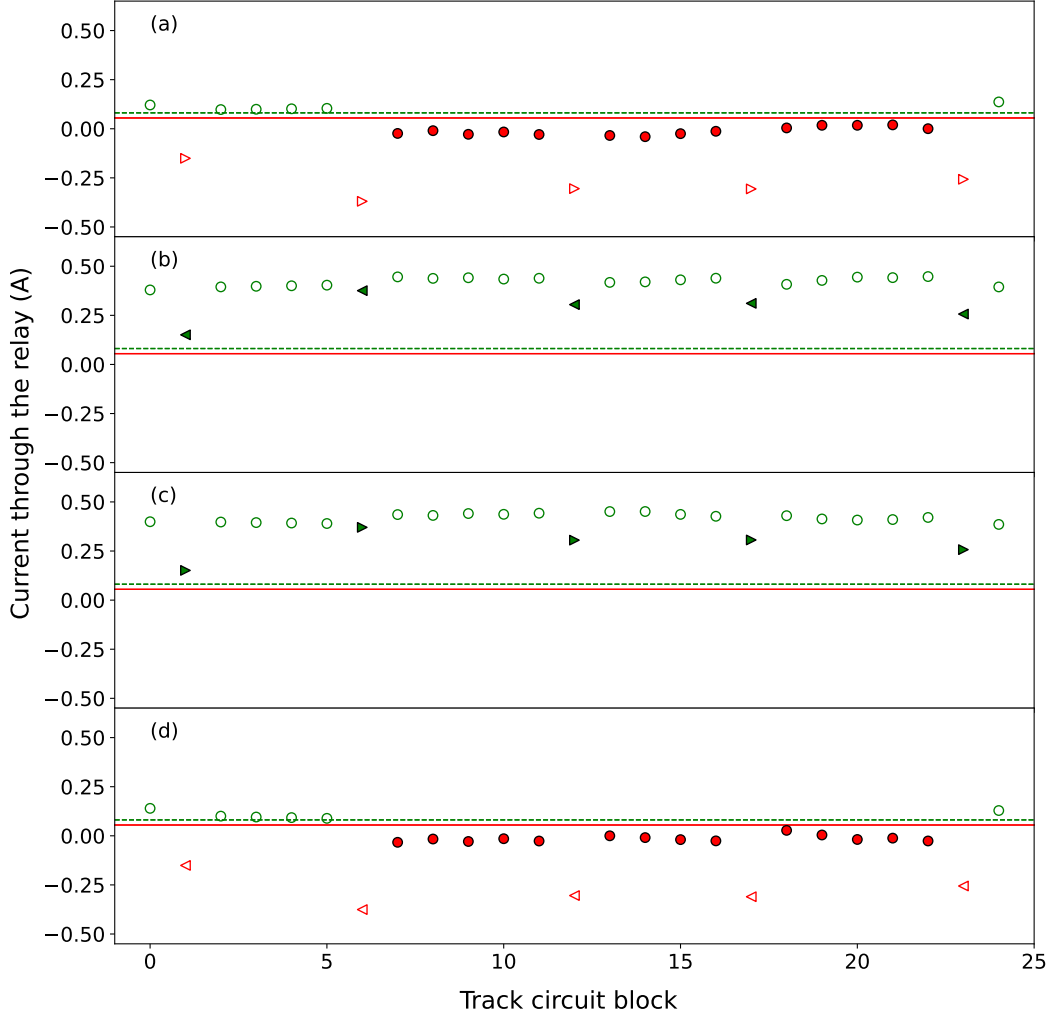
Figure 19. Preston to Lancaster: The current through each relay at the 1-in-100 year extreme geoelectric field estimate of $E_x = 5\,\mathrm{V\,km^{-1}}$ in the (a) northwards and (b) southwards directions of travel, and $E_x = -5\,\mathrm{V\,km^{-1}}$ in (c) northwards and (d) southwards directions of travel. The red (solid) line is the 'drop-out current' the value below which the current must drop to de-energise the relay, turning the signal red; the green (dashed) line is the 'pick-up current', the value above which the current must rise to energise the relay, turning the signal green. A green ring with no fill indicates an unoccupied block operating normally, and a red triangle with no fill is an occupied block operating normally, with the direction of the triangle showing the direction of travel (right for northwards and left for southwards). A filled green triangle indicated a "wrong side" failure, and a filled red circle is a "right side" failure. Here we see both types of misoperation occurring in both directions depending on the orientation of the electric field.

5 Discussion

The model used in this study builds upon the work set out in P23. With the addition of cross bonds linking together both directions of travel in the line, and train axles to allow the study of "wrong side" failures, we further improve the realism of the model, and the scope of the investigation into the impacts of space weather on railway signaling systems in the United Kingdom. The continued usage of Network Rail standards documents ensures we are using appropriate parameters for the UK case, but even the UK network is not homogeneous, so the model is designed to be easily adapted to different rail and track circuit parameters. The model could therefore be used to study railway networks in other countries also with minimal effort provided the data is easily accessible, which is not always the case.

Comparison of our results with the electric field and horizontal magnetic field change statistics from Beggan et al. (2013) and Rogers et al. (2020) shows that wrong side failures would occur in events that occur once every 10-20 years. Comparing the threshold electric field to cause "wrong side" failures in this study to the threshold for "right side" failures in P23, it is apparent that the strength of the electric field needed to cause a "wrong side" failure is lower than is needed to cause a "right side" failure. To cause a "wrong side" failure, due to the train axles cutting off the power supply, the current flowing through the relay is almost entirely the induced current from the electric field. However, in the case of "right side" failure, for the induced current to de-energise the relay, it must overcome the current already present in the circuit from the power supply. It is this difference in current that is responsible for the different threshold values for misoperation.

While it is important to consider the electric field strength threshold for "wrong side" failures, at the same time we need to consider the conditions that need to be met for these misoperations to occur and consider the likelihood. Firstly, a train must occupy the block in question, this might not always be the case, as peak electric fields generated during a geomagnetic storm may occur overnight when traffic is less dense. Secondly, the train must be sufficiently far along the line, such that the minimum length of track needed to build-up the required amount of current to cause a "wrong side" failure is between the rear axle of the train and the relay.

It is challenging to determine which type of misoperation is dominant. The thresholds for "wrong side" failures are lower, but they depend on the multiple factors described above happening simultaneously for misoperation to take place. In contrast, the conditions for right-side failures to occur are simpler, but a higher electric field strength is needed for misoperation to occur.

The study has centered on geoelectric fields that have a fixed direction and magnitude, although in actuality, they tend to fluctuate in intensity and direction over time. The effects of time-varying fields requires further investigation. For instance, it is unclear how long geoelectric fields must maintain a particular strength and/or orientation to trigger a misoperation. In such scenarios, it will also be necessary to analyze the response times of different track circuit types to changes in current to analyze the susceptibility.

It is also important to point out that in the event of severe space weather, railway signaling will not be the only system affected. Power supply networks, communications, Global Navigation Satellite Systems (GNSS) are all susceptible, many of which will also impact the safe and smooth operation of the railway network, regardless of the countless other affects to other areas. Further study needs to focus on the connectivity of these systems, and how sectors as a whole could be affected by the loss of interdependent systems Darch et al. (2014); Hapgood et al. (2021).

6 Conclusion

This study shows the results of a realistic model of geomagnetic interference in DC signaling systems on AC-electrified railway lines. Built upon the model detailed in P23, we now have the ability to study both directions of travel simultaneously, electrically bonded with cross bonds, and to consider "wrong side" failures - when train axles bypass the relays and de-energising them, but geomagnetically induced currents cause the relays to re-energise and display the wrong signal.

We have shown that the susceptibility of a track circuit to experience a "wrong side" failure is strongly dependent on the location of the train within the track circuit block, where the risk of misoperation increases as the distance between the train and the relay increases. It was also demonstrated that the presence of trains in a block has very little impact on the current across the relays of nearby unoccupied blocks in both directions of travel.

It was found that the threshold electric field strength for "wrong side" failure along this line was $E_y = -1\,\mathrm{V\,km^{-1}}$ for the eastwards direction of travel and $E_y = 1\,\mathrm{V\,km^{-1}}$ for the westwards direction of travel. This corresponds to an estimate for the electric field strength of events that occur once in a decade or two. The "wrong side" failure threshold electric field strength is lower than the threshold for "right side" failure along the same line.

A uniform electric field with a magnitude of $4\,\mathrm{V\,km^{-1}}$, a value that is known to have caused misoperations in the past, was applied to the section being studied, with 55 of the 70 track circuits having the potential to experience "wrong side" failures. It was also shown that you would see both "wrong side" and "right side" failures in opposite directions of travel.

Applying an electric field with a magnitude of $5\,\mathrm{V\,km^{-1}}$, which is the estimate for a 1-in-100 year extreme event in the UK, we saw that the number of track circuits with the potential to experience "wrong side" failures increased very slightly, while the number of "right side" failures increased a greater extent.

7 Open Research

Network Rail standard documents can be obtained from `https://global.ihs.com/csf_home.cfm?&csf=NR`. Data used for modeling are available at DOI: available at publication.

References

Alm, E. (1956). Measures against geomagnetic disturbances in the entire dc track circuit for automatic signalling systems, original publication (in swedish) appendix 5f, betänkande: angående det tekniska utförandet av signalanläggningar vid statens järnvägar, 1956. Translation (in English), June 2020. *Infrastructure Resilience Risk Reporter*, *1*, 28-51. Retrieved from `https://carleton.ca/irrg/journal/`

Beggan, C. D., Beamish, D., Richards, A., Kelly, G. S., & Alan, A. W.   (2013).   Prediction of extreme geomagnetically induced currents in the UK high-voltage network. *Space Weather*, *11*, 407-419. doi: 10.1002/swe.20065

Boteler, D. H. (2021). Modeling geomagnetic interference on railway signaling track circuits. *Space Weather*, *19*. doi: 10.1029/2020SW002609

Boteler, D. H., & Pirjola, R. J.   (2019).   Numerical calculation of geoelectric fields that affect critical infrastructure.   *International Journal of Geosciences*, *10*, 930-949. doi: 10.4236/ijg.2019.1010053

Boteler, D. H., & Trichtchenko, L.   (2015).   Telluric influence on pipelines.   In R. W. Revie (Ed.), *Oil and gas pipelines: Integrity and safety handbook* (p. 275-288). John Wiley and Sons, Inc. doi: 10.1002/9781119019213.ch21

Cabinet Office.   (2012).   *National risk register of civil emergencies.*   22 Whitehall, London, SW1A 2WH.

Darch, G., McCormack, L., Hayes, D., Tomlinson, J., Hooper, P., Williams, R., . . . Tyndall, M.   (2014).   *Rail resilience to space weather final phase 1 report department for transport* (Tech. Rep.).   Western House (Block B), Peterborough Business Park, Lynch Wood, Peterborough, PE2 6FZ: Atkins Limited.

Eroshenko, E. A., Belov, A. V., Boteler, D., Gaidash, S. P., Lobkov, S. L., Pirjola, R., & Trichtchenko, L.   (2010).   Effects of strong geomagnetic storms on northern railways in russia.   *Advances in Space Research*, *46*, 1102-1110.   doi: 10.1016/j.asr.2010.05.017

Hapgood, M., Angling, M. J., Attrill, G., Bisi, M., Cannon, P. S., Dyer, C., . . . Willis, M.   (2021).   Development of space weather reasonable worst-case scenarios for the uk national risk assessment.   *Space Weather*, *19*.   doi: 10.1029/2020SW002593

Iwasaki, M., Furukawa, K., Okamoto, K., Koreishi, K., Kaneyasu, T., Kota, Y., . . . Radford, A.   (2017).   Development of class 385 semi-customised/standard commuter rolling stock for global markets. *Hitachi Review*, *66*.

Kasinskii, V. V., Ptitsyna, N. G., Lyahov, N. N., Tyasto, M. I., Villoresi, G., & Iucci, N.   (2007).   Effect of geomagnetic disturbances on the operation of railroad automated mechanisms and telemechanics. *Geomagnetism and Aeronomy*, *47*, 676-680. doi: 10.1134/S0016793207050179

Krausmann, E., Andersson, E., Russell, T., & Murtagh, W.   (2015).   *Space weather and rail: Findings and outlook* (Tech. Rep.).   Joint Research Centre, Via E. Fermi 2749, 21027 Ispra (VA), Italy: European Commission.   Retrieved from https://ec.europa.eu/jrc doi: 10.2788/211456

Lejdström, B., & Svensson, S. (1956). Calculation of geomagnetic interference voltages in track circuits, original publication (in swedish) appendix 6, betänkande: angående det tekniska utförandet av signalanläggningar vid statens järnvägar, 1956. Translation (in English) June 2020.   *Infrastructure Resilience Risk Reporter*, *1*, 28-51. Retrieved from https://carleton.ca/irrg/journal/

Lewis, Z. M., Wild, J. A., Allcock, M., & Walach, M. T.   (2022).   Assessing the impact of weak and moderate geomagnetic storms on UK power station transformers. *Space Weather*, *20*. doi: 10.1029/2021SW003021

NR/GN/ELP/27312. (2006). *Impedances of 25 kv a.c. overhead lines for classic system* (Tech. Rep.). 40 Melton Street, London, NW1 2EE: Network Rail.

NR/SP/ELP/21085. (2007). *Specification for the design of earthing and bonding systems for the 25 kv a.c. electrified lines* (Tech. Rep.). 40 Melton Street, London, NW1 2EE: Network Rail.

NR/SP/SIG/50004. (2006). *Methodology for the demonstration of electrical compatibility with dc (ac immune) track circuits* (Tech. Rep.). 40 Melton Street, London, NW1 2EE: Network Rail.

Patterson, C. J., Wild, J. A., & Boteler, D. H.   (2023).   Modeling the impact of geomagnetically induced currents on electrified railway signalling systems in the United Kingdom. *Space Weather*. doi: 10.1029/2022SW003385

Pirjola, R.   (1985).   On currents induced in power transmission systems during geomagnetic variations.   *IEEE Transactions on Power Apparatus and Systems*, *PAS-104*, 2825-2831. doi: 10.1109/TPAS.1985.319126

Ptitsyna, N. G., Kasinskii, V. V., Villoresi, G., Lyahov, N. N., Dorman, L. I., & Iucci, N.   (2008).   Geomagnetic effects on mid-latitude railways: A statistical study of anomalies in the operation of signaling and train control equipment on the east-siberian railway. *Advances in Space Research*, *42*, 1510-1514.   doi: 10.1016/j.asr.2007.10.015

Pulkkinen, A., Viljanen, A., Pajunpää, K., & Pirjola, R.   (2002).   Recordings and occurrence of geomagnetically induced currents in the Finnish natural gas pipeline network. *Applied Geophysics*, *48*.

Rogers, N. C., Wild, J. A., Eastoe, E. F., Gjerloev, J. W., & Thomson, A. W.   (2020).   A global climatological model of extreme geomagnetic field fluctuations.   *Journal of Space Weather and Space Climate*, *10*.   doi: 10.1051/swsc/2020008

Wik, M., Pirjola, R., Lundstedt, H., Viljanen, A., Wintoft, P., & Pulkkinen, A.   (2009).   Space weather events in july 1982 and october 2003 and the effects of geomagnetically induced currents on swedish technical systems.   *Annales Geophysicae*, *27*, 1775-1787.